



ELECTROCHEMICAL SYNTHESIS OF HEXAGONAL HOLLOW ZnO NANOSTRUCTURES

¹Abellán, M., ²Moya, M. and ^{2,*}Marí, B.

¹Instituto de Química, Facultad de Ciencias, Pontificia Universidad Católica de Valparaíso, Av. Universidad 330, Curauma Valparaíso, Chile

²Departament de Física Aplicada-IDF. Universitat Politècnica de València, Camí de Vera s/n, 46022, València, Spain

ARTICLE INFO

Article History:

Received 28th December, 2014
Received in revised form
08th January, 2015
Accepted 20th February, 2015
Published online 17th March, 2015

Key words:

ZnO, Nanotubes,
Electrodeposition.

ABSTRACT

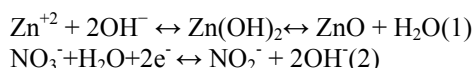
A simple and controllable one-step electrode position process is proposed in order to obtain ZnO nanotubes. Zinc oxide thin films were grown on fluorine-doped tin oxide by electrode position from an aqueous electrolyte containing zinc nitrate and potassium nitrate. Generally, in aqueous electrolytes ZnO is electrochemically deposited in the form of hexagonal nanocolumns. These nanocolumns grow perpendicularly to the substrate until reaching a maximum height of about 2 μm and then the perpendicular growth vanishes and the solid nanocolumns develop to hexagonal hollow structures. Several characteristics of the electrodeposited films such as thickness, morphology and crystalline structure were obtained as a function of the deposited charge. The evolution of the morphology of the electrodeposited layers as a function of time was monitored by Scanning Electron Microscopy. X-Ray Diffraction confirms that hexagonal nanotubes are preferentially oriented along the (002) direction.

Copyright © 2015 Abellán et al. This is an open access article distributed under the Creative Commons Attribution License, which permits unrestricted use, distribution, and reproduction in any medium, provided the original work is properly cited.

INTRODUCTION

ZnO has aroused an enormous interest in recent years due to its wide band gap (3.3 eV) and large exciton binding energy (60 meV), which stimulate its use in optoelectronic devices (working on the blue and ultraviolet wavelength regions) (Volk et al 2008), chemical sensors (Park et al., 2008), piezoelectric transducers (Aeugle et al., 1991) and so on. More recently, its application in energy conversion has been the subject of intense research due to the possibility to be used in Dye Sensitized Solar Cells (DSSC) (Suri et al., 2007; Keis et al., 2002) as a good alternative to TiO₂. As far as the growth method is concerned, there are multiple ways of obtaining thin films, such as chemical vapor deposition (VPD) (Liu et al., 2009), Metalorganic Chemical Vapor Deposition (MOVPE) (Kasuga et al., 2005), spray pyrolysis (Bian et al., 2008), sputtering (Water et al., 2002), Molecular Beam Epitaxy (MBE) and pulsed laser deposition (PLD) (Sun et al., 2004). However, among these possibilities, the growth of ZnO films by electrodeposition techniques has been considered the most suitable in the manufacturing of thin films for application, which require the development on a simple and efficient growth method. The advantage of this technique is related to its flexibility, the control of the process parameters, as well as its adaptability to industrial process. Additionally,

it is a uniquely low cost technique ideal for obtaining thin films like ZnO semiconductors. The influence of the concentration of salts in the electrolyte bath is the key to obtaining transparent ZnO semiconductors using nitrate salts. Further vertically ZnO nanostructures can be grown by cathodic electrodeposition from aqueous electrolytes containing nitrate salts. The process implies the formation of hydroxyl ions at the surface of the films. In this way, the deposition process of zinc hydroxide from zinc nitrate solution is based on the reduction of the nitrate, according to the following reaction:



The hydroxyl ions react with Zn ions present in the solution to form spontaneously more stable ZnO by means of the dehydrated zinc hydroxide at high temperatures (>50°C) (Peulon et al., 1998). This electrodeposition process leads to polycrystalline films with high crystalline quality, with the columnar structures its typical morphology. Equation (2) refers to electrochemical reduction of nitrate ions, which are controlled by both the concentration and potential deposition bath (Manzano et al., 2011). Some authors reported the generation of ZnO nanotubes through a 3 steps electrochemical procedure consisting of an initial electrodeposition of ZnO nanocolumns followed by a chemical etching and a subsequent electrochemical regrowth (Cembrero et al., 2013).

*Corresponding author: Marí, B.

Departament de Física Aplicada-IDF. Universitat Politècnica de València, Camí de Vera s/n, 46022, València, Spain.

In this paper we report an alternative method for obtaining hexagonal hollow structures based on ZnO by means of one-step electrodeposition. The thicknesses of ZnO thin films, which are proportional to the height of nanocolumns, were monitored as a function of deposited charge. Increasing the deposited charge results in higher nanocolumns, reaching up to heights of about 2 μm . For deposited charges higher than 4 C/cm^2 the nanocolumns develop into nanotubes. The formation of ZnO hexagonal nanocolumns and subsequent transformation into nanotubes were followed by performing SEM and XRD measurements at different stages of the growth.

Experimental section

The cathodic electrodeposition process was performed with a standard electrochemical cell with a three electrode configuration: a commercial conducting glass substrate, Fluorine-doped Tin Oxide (FTO) coated glass with a $\sim 10\Omega/\square$ sheet resistance as cathode (work electrode), a Pt mesh as anode (counter electrode) and an Ag/AgCl reference electrode ($E_0 = +222$ mV vs Normal Hydrogen Electrode, NHE). The cell was controlled with a potentiostat / galvanostat Autolab connected to a computer. The ZnO thin films were electrodeposited in a solution of zinc nitrate and potassium nitrate salts. The electrolyte contained a mixture of 0.1 M KNO_3 ($\geq 99\%$, PanreacQuímica S.A.U) in de-ionized water ($0.05 \mu\text{S}$) and 5×10^{-3} M $\text{Zn}(\text{NO}_3)_2$ ($\geq 99\%$, Fluka). The pH of the solution was 4.85. The electrolyte was purged with N_2 at volume flow rate of 200 mL/min while stirring, by using of a magnetic bar stirrer, in order to facilitate the N_2 diffusion. Before the electrodeposition process, the FTO glass was cleaned in ethanol for 15 min, and subsequently in acetone 15 min and then rinsed with de-ionized water. The films were growth potentiostatically at -0.96 V in a thermostatic bath at 80°C with a thermal stability of $\pm 1^\circ\text{C}$. For ZnO thin film with $\sim 1 \mu\text{m}$ thick, the time deposition was between 1400 - 2000 s. After the deposition, the ZnO films were cleaned with water and finally dried in air at room temperature. The surface of the deposited layer always fitted 1 cm^2 .

ZnO physical properties were investigated by combining morphological and structural techniques. The morphological characterization of the films was performed by JEOL-JSM6300 Scanning Electron Microscope (SEM) operating at 20kV. The structural characterization was carried out by high-resolution X-ray diffraction (XRD) using a Rigaku Ultima IV diffractometer in θ - 2θ mode with a copper cathode ($\text{CuK}\alpha$, 1.5418 \AA) operating at 40 kV and 40 mA. The diffraction pattern was scanned between 25° and 75° (2θ) in steps of 0.02° . The thicknesses of the deposited films were measured with respect to the substrate using a Veeco profilometer Dektak 150.

RESULTS AND DISCUSSION

ZnO thickness as function of the charge deposited

Figure 1 shows the thickness of ZnO thin films synthesized from the mentioned nitrate electrolyte as a function of the deposited charge.

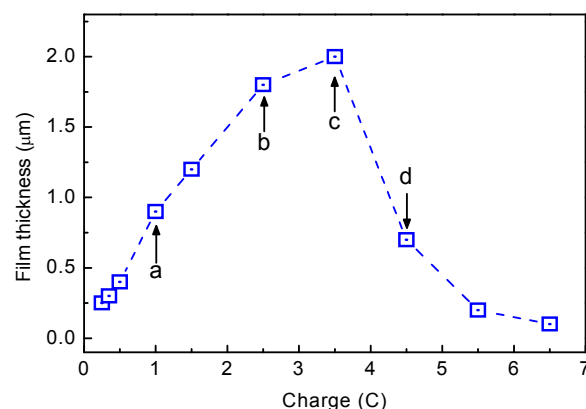


Figure 1. Evolution of thin film thickness versus accumulated charge deposited from an aqueous electrolyte containing $[\text{Zn}(\text{NO}_3)_2]=5 \text{ mM}$ and $[\text{KNO}_3]=0.1 \text{ M}$

A progressive increase of the films' thickness is expected when increasing the deposited charge. In this case the thickness of ZnO thin films, which is directly related to the height of the nanocolumns, increases linearly with the deposited charge reaching a maximum thickness of 2 μm for a deposited charge of 3.5 C/cm^2 . A higher amount of deposited charge results in progressively thinner films, up to the point of practically vanishes at a deposited charge of 7 C/cm^2 . This effect is assigned to the coexistence of two competing mechanisms described by equation (1). Equation (1) takes place in both senses, so the Zn^{2+} cations present in the electrolyte are combined with OH^- anions resulting in intermediate ZnO hydroxide and finally ZnO crystals. Then the reverse mechanism consists in the dissolution of ZnO in water resulting in intermediate ZnO hydroxide molecules, which decompose in Zn cations and OH^- anions, respectively. The two competing mechanisms, generation and dissolution of ZnO, impedes the growth of ZnO films thicker than 2 microns, at least when FTO substrates are used.

ZnO film growth study

The SEM micrographs of Figure 2 belong to ZnO films deposited at different deposited charges ranging from -1 to $-4.5 \text{ C}/\text{cm}^2$. When the accumulated charge reaches $-1 \text{ C}/\text{cm}^2$ (Fig.2a) the film exhibits uniform morphology of oriented hexagonal nanocolumns. The nanocolumns does not cover entirely the whole surface of the substrate and some voids are still observed. A deposited charge close to $-2 \text{ C}/\text{cm}^2$ is required to achieve a complete recovery of the FTO substrate. For charges of about $-2.5 \text{ C}/\text{cm}^2$ (Fig.2b) the films are formed by columns of different sizes compactly packet but still with some pores appearing among these packets. This growth may be associated with a rise of the Zn^{2+} concentration in the bath solution. Zn^{2+} ions reduce the nitrate ions and promote the zinc hydroxide formation.

For charges of about $-3.5 \text{ C}/\text{cm}^2$ (Fig.2c) the radii of hexagonal columns increases and columns becomes wider. At this deposited charges the substrate is completely recovered. Additionally, an enhancement in the pores concentration can be appreciated. Finally, for deposited charges of about $-4.5 \text{ C}/\text{cm}^2$ (Fig. 2d), hollow hexagonal column structures are obtained. This can be interpreted by assuming that equation (1) and (2),

related to the formation and destruction of ZnO nanostructures, are both reversible and are taking place simultaneously. In the beginning of the electrode position process the formation of ZnO nanocolumns is the dominant process. When the ZnO nanostructures are already formed the reverse process becomes more important, resulting in the destruction of the nanocolumns. This process starts for the 002 planes because they are weaker than the perpendicular planes, which results in the formation of nanotubes.

the samples the peak is slightly displaced to the left, pointing towards a change in the stress state of the films, towards a tensile stress. Also the FWHM (Full Width at Half Maximum) for the preferential (002) peak was calculated, in order to assess the crystalline quality of these thin films. The FWHM values as a function of the accumulated charge is shown in the Figure 4. The grain size of the films rises when the accumulated charge increases. In this case the biggest grain sizes were obtained for samples with accumulated charge of -3.5 C/cm^2 .

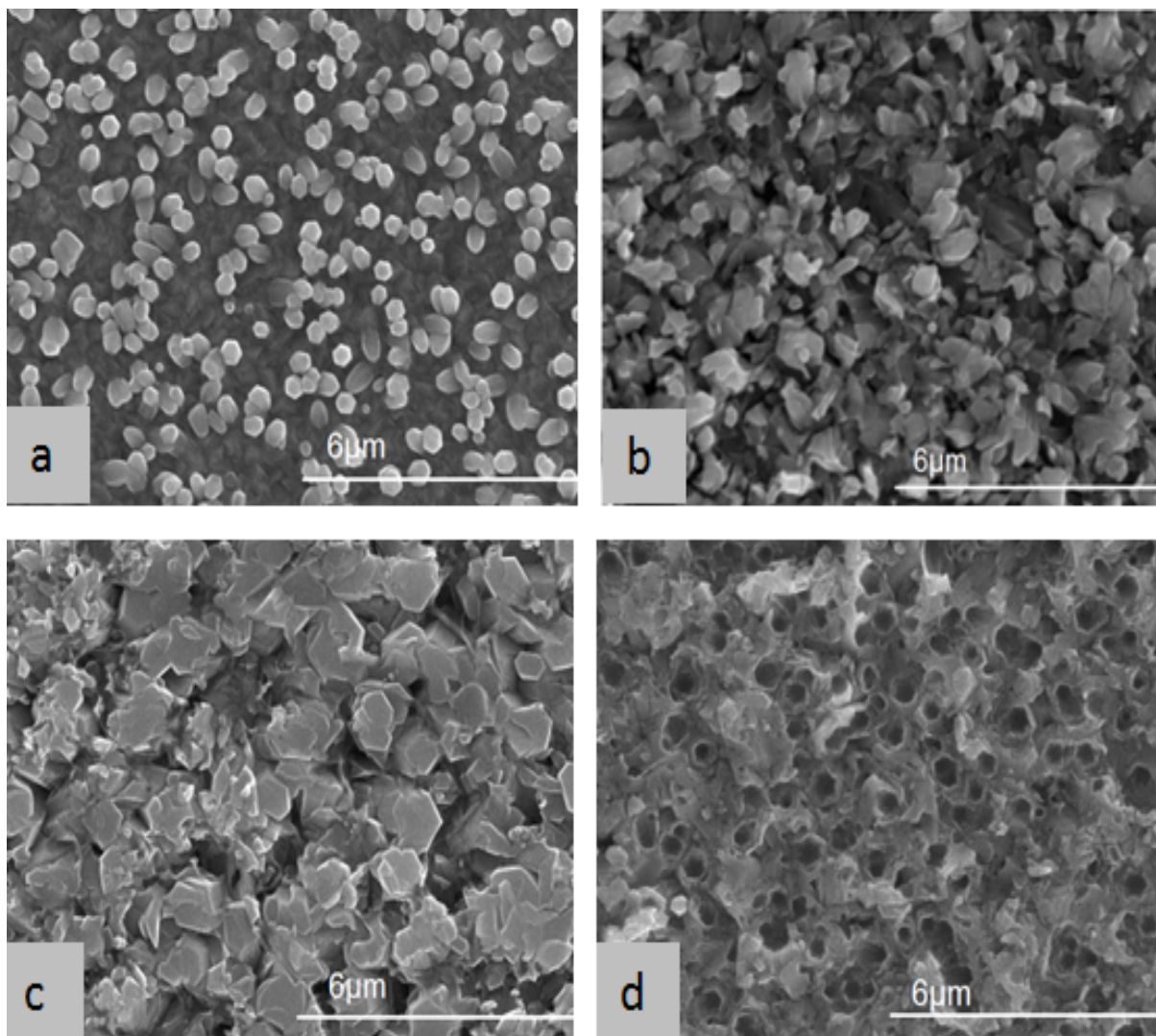


Figure 2. SEM micrographs of several ZnO thin films electrodeposited on FTO substrates from aqueous electrolyte containing 5 mM of $[\text{Zn}(\text{NO}_3)_2]$ and 0.1 mM of $[\text{KCl}]$ for different deposited charge: -1C (a), -2.5C (b), -3.5C (c) and -4.5C (d)

Crystallinity

The crystal structure was studied by XRD in the Bragg-Brentano geometry. Figure 3 shows the diffraction patterns of the samples, which SEM micrographs are shown in Figure 2. Six diffraction peaks located approximately at 31.73° , 34.44° , 36.21° , 47.42° , 56.54° and 62.76° which are related to the (100), (002), (101), (102), (110) and (103) crystallographic directions, respectively, are observed. Thus, these results show that samples are polycrystalline with a preferential orientation along the (002) direction. Considering the (002) peaks and comparing its position with that of JCCD-036-1451, one realize that for all

As mentioned above at deposited charge higher than -3.5 C/cm^2 the reverse reaction dominates and the destruction of nanocolumns takes place. Initially, the weakest crystallographic planes (002) are affected by reverse reactions and the nanocolumns become hollow and then the rest of the faces are also damaged.

This damage modifies the crystal and results in a reduction of grain size observed by XRD for deposited charge higher than -3.5 C/cm^2 .

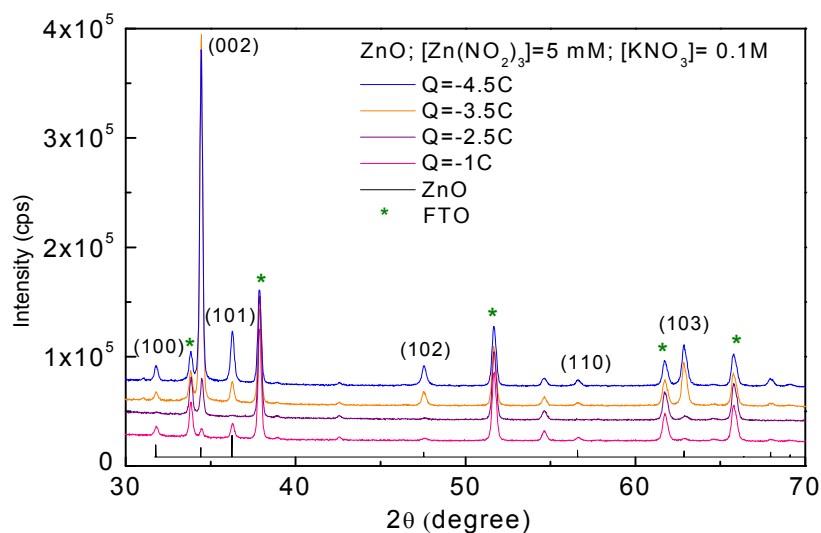


Figure 3. XRD patterns of ZnO thin films for different deposited charge

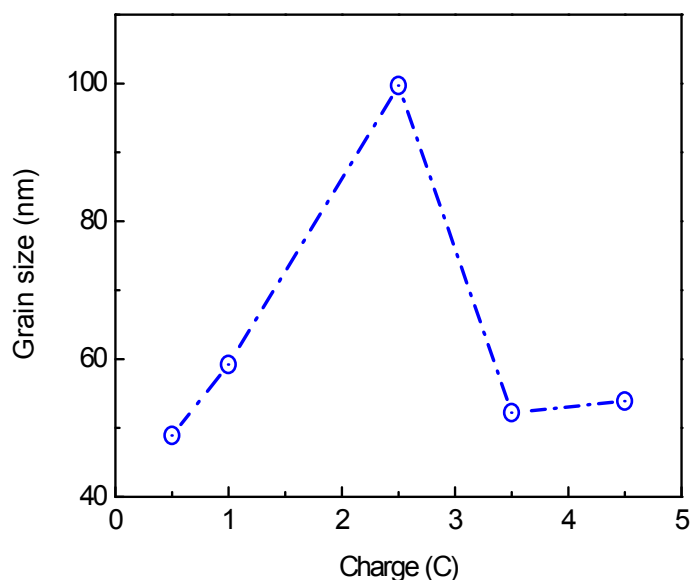


Figure 4. Evolution of FWHM versus accumulated charge

Conclusion

ZnO hexagonal nanotubes on FTO were grown by cathodic electrodeposition technique in a one-step procedure. The aqueous electrolyte was composed by a mix of nitrates; $\text{Zn}(\text{NO}_3)_2$ and KNO_3 . Hexagonal ZnO columns are formed in the first stages and then nanotubes are promoted due to the etching of ZnO columns. We conclude that two mechanisms related to growth and etching, respectively, are always in competition. The coexistence of two competing mechanisms impedes obtaining electrodeposited layers thicker than $2 \mu\text{m}$, at least in FTO substrates.

Acknowledgments

This work was supported by CONICYT (project 3130451), Ministerio de Economía y Competitividad (project ENE2013-

46624-C4-4-R) and European Commission through NanoCIS project FP7-PEOPLE-2010-IRSES (ref. 269279).

REFERENCES

- Aeugle, Th, Bialas, H., Henekam K. and Pleyerm, W. 1991 Large area piezoelectric ZnO film transducers produced by r.f. diode sputtering. *Thin Solid Films*; 201:293-304.
- Bian, J. M, Li, X. M, Gao, X. D, Yu, W. D. and Chen, L. D. 2004 Electronic Structure and Optical Properties of Vertically Aligned ZnO Nanorod Arrays Grown by Low temperature Hydrothermal Method. *Applied Physics Letters*; 84:541-543.
- Cembrero, J., Busquets-Mataix, D., Rayón, E., Pascual, M., Pérez Puig, M. A. and Marí, B. 2013. Control parameters

- on the fabrication of ZnO hollow nanocolumns. *Materials Science in Semiconductor Processing* ;16:211-216
- Kasuga, M., Takano, T., Akiyama, S., Hiroshima, K., Yano, K. and Kishiom K. 2005 Growth of ZnO films by MOCVD in high magnetic field. *Journal of Crystal Growth* ;275:e1545-e1550.
- Keis, K., Magnusson, E., Lindstrom, H., Lindquist, S. E, Hagfeldt, A. A. 2002. 5% efficient photo electrochemical solar cell based on nanostructured ZnO electrodes. *Solar Energy Materials and Solar Cells.*;73:51–58.
- Liu, B. and Zeng, H. C. 2009 Direct growth of enclosed ZnO nanotubes. *Nano Res*;2:201-209.
- Manzano, C. V., Alegre, D., Caballero-Calero, O., Alén B. and Martín-González M. S. 2011. Synthesis and luminescence properties of electrodeposited ZnO Films. *Journal of Applied Physics*. 110:043538-1-043538-8
- Park, J. Y., Song, D. E. and Kim, S. S. 2008. An approach to fabricating chemical sensors based on ZnO nanorod arrays. *Nanotechnology* ;19:105503.
- Peulon, S. and Lincot, D. 1998. Mechanistic Study of Cathodic Electrodeposition of Zinc Oxide and Zinc Hydroxychloride Films from Oxygenated Aqueous Zinc Chloride Solutions. *Journal of Electrochemical Society*;145:864-874
- Sun, Y, Fuge, G. M. and Ashfold, M. N. R. 2004 Growth of aligned ZnO nanorod arrays by catalyst-free pulsed laser deposition methods. *Chemical Physics Letters*;396:21-26.
- Suri, P, Panwar, M, Mehra, R, M. 2007 Photovoltaic performance of dye-sensitized ZnO solar cell based on Eosin- Y photosensitizer. *Materials Science-Poland* ;25:137-144.
- Volk, J., Håkansson, A., Miyazaki, H. T., Nagata, T, Shimizu, J. and Chikyow, T. 2008 Fully engineered homoepitaxial zinc oxide nanopillar array for near-surface light wave manipulation. *Appl Phys Lett* ;92:183-114.
- Water, W. and Chu, S. Y. 2002 Physical and structural properties of ZnO sputtered films. *Materials Letters*;55:67-72.
